On the Orientation of a Designed Transmembrane Peptide: Toward the Right Tilt Angle?

4 AUTHORS, INCLUDING:

Catherine Etchebest
French Institute of Health and Medical Resea…
33 PUBLICATIONS **656** CITATIONS

Josephine Antoinette Killian
Utrecht University
166 PUBLICATIONS **8,634** CITATIONS

On the Orientation of a Designed Transmembrane Peptide: Toward the Right Tilt Angle?

Suat Özdirekcan,[‡] Catherine Etchebest,[†] J. Antoinette Killian,[‡] and Patrick F. J. Fuchs*,[†]

Contribution from the Department of Chemical Biology and Organic Chemistry, Bijvoet Center for Biomolecular Research, Utrecht University, Padualaan 8, 3584 CH Utrecht, The Netherlands, and Equipe de Bioinformatique Génomique et Moléculaire INSERM UMR-S 726, Université Paris-Diderot-Paris 7, Case Courrier 7113, 2, place Jussieu, 75251 Paris Cedex 05, France

Received May 25, 2007; E-mail: Patrick.Fuchs@ebgm.jussieu.fr

Abstract: The orientation of the transmembrane peptide WALP23 under small hydrophobic mismatch has been assessed through long-time-scale molecular dynamics simulations of hundreds of nanoseconds. Each simulation gives systematically large tilt angles ($>30°$). In addition, the peptide visits various azimuthal rotations that mostly depend on the initial conditions and converge very slowly. In contrast, small tilt angles as well as a well-defined azimuthal rotation were suggested by recent solid-state ^2H NMR studies on the same system. To optimally compare our simulations with NMR data, we concatenated the different trajectories in order to increase the sampling. The agreement with ^2H NMR quadrupolar splittings is spectacularly better when these latter are back-calculated from the concatenated trajectory than from any individual simulation. From these ensembled-average quadrupolar splittings, we then applied the GALA method as described by Strandberg et al. (*Biophys. J.* **2004**, *86*, 3709−3721), which basically derives the peptide orientation (tilt and azimuth) from the splittings. We find small tilt angles ($6.5°$), whereas the real observed tilt in the concatenated trajectory presents a higher value ($33.5°$). We thus propose that the small tilt angles estimated by the GALA method are the result of averaging effects, provided that the peptide visits many states of different azimuthal rotations. We discuss how to improve the method and suggest some other experiments to confirm this hypothesis. This work also highlights the need to run several and rather long trajectories in order to predict the peptide orientation from computer simulations.

Introduction

A large variety of cellular processes involves membrane proteins. A majority of these membrane proteins have one or more of their hydrophobic segments crossing the lipid bilayer, and thereby are in contact with the lipid acyl chains and headgroups. Typically, membrane-spanning protein segments consist of α-helical stretches of 20−22 hydrophobic residues flanked by polar or aromatic residues, approximately matching the hydrophobic thickness of biomembranes.[1−6] It has been well documented that the structure and activity of integral proteins can be influenced by the extent of mismatch between the hydrophobic length of transmembrane segments of a protein and the hydrophobic thickness of a lipid bilayer,[7−9] whereby

also the interactions of the flanking residues with the lipid−water interface can play an important role.[10,11]

In order to study how the structural and/or dynamic properties of membrane proteins are influenced by the interactions with the surrounding lipids, several groups used designed α-helical peptides that mimic the transmembrane segments of proteins in synthetic lipid bilayers.[11−17] Examples are the so-called WALP and KALP peptides, which are composed of leucine-alanine repeats with variable lengths that are flanked on both sides by Trp and Lys residues, respectively.[13,14] These peptides were used to investigate the role of interfacial interactions in membrane organization by studying the consequences of the hydrophobic mismatch between the hydrophobic lengths of the peptides and lipid acyl chains.[13,14] In the case of WALP peptides

‡ Utrecht University.

† Université Paris-Diderot-Paris 7.

(1) Isaiah, T.; Arkin, I. T.; Brunger, A. T. *Biochim. Biophys. Acta* **1998**, *1429*, 113−128.
(2) Landolt-Marticorena, C.; Williams, K. A.; Deber, C. M.; Reithmeier, R. A. *J. Mol. Biol.* **1993**, *229*, 602−608.
(3) Reithmeier, R. A. *Curr. Opin. Struct. Biol.* **1995**, *5*, 491−500.
(4) Sakai, H.; Tsukihara, T. *J. Biochem. (Tokyo)* **1998**, *124*, 1051−1059.
(5) von Heijne, G. *Annu. Rev. Biophys. Biomol. Struct.* **1994**, *23*, 167−192.
(6) Wallin, E.; Tsukihara, T.; Yoshikawa, S.; von Heijne, G.; Elofsson, A. *Protein Sci.* **1997**, *6*, 808−815.
(7) Dumas, F.; Lebrun, M. C.; Tocanne, J. F. *FEBS Lett.* **1999**, *458*, 271−277.
(8) Killian, J. A. *Biochim. Biophys. Acta* **1998**, *1376*, 401−415.
(9) Lee, A. G. *Biochim. Biophys. Acta* **2003**, *1612*, 1−40.

(10) de Planque, M. R.; Killian, J. A. *Mol. Membr. Biol.* **2003**, *20*, 271−284.
(11) Demmers, J. A.; van Duijn, E.; Haverkamp, J.; Greathouse, D. V.; Koeppe, R. E., II; Heck, A. J.; Killian, J. A. *J. Biol. Chem.* **2001**, *276*, 34501−34508.
(12) Davis, J. H.; Clare, D. M.; Hodges, R. S.; Bloom, M. *Biochemistry* **1983**, *22*, 5298−5305.
(13) de Planque, M. R.; Bonev, B. B.; Demmers, J. A.; Greathouse, D. V.; Koeppe, R. E., II; Separovic, F.; Watts, A.; Killian, J. A. *Biochemistry* **2003**, *42*, 5341−5348.
(14) Killian, J. A. *FEBS Lett.* **2003**, *555*, 134−138.
(15) Killian, J. A.; Nyholm, T. K. *Curr. Opin. Struct. Biol.* **2006**, *16*, 473−479.
(16) Ren, J.; Lew, S.; Wang, J.; London, E. *Biochemistry* **1999**, *38*, 5905−5912.
(17) Zhang, Y. P.; Lewis, R. N.; Hodges, R. S.; McElhaney, R. N. *Biochemistry* **1995**, *34*, 2362−2371.

that have a hydrophobic length longer than the hydrophobic thickness of the lipid bilayer (i.e., positive mismatch), several responses to mismatch were observed. ^{2}H NMR experiments on acyl-chain-deuterated diacylphosphatidylcholine (PC) lipids showed small but systematic increases in acyl chain order, indicating a stretching of the lipids with increasing mismatch.[13,18] ^{2}H NMR experiments on the 23-amino-acids-long peptide WALP23 that was deuterated on alanine side chains demonstrated, in addition, a small but systematic increase in the tilt angle of WALP23 with increasing hydrophobic mismatch.[19] Control experiments with the corresponding lysine-flanked peptide KALP23 showed a different response. In this case, no significant stretching of the lipids was observed, the tilt angle was slightly larger than for WALP23, and the direction of the tilt was very different.[20] In these ^{2}H NMR studies, the tilt angle was determined indirectly from the experimental quadrupolar splittings (QS), using the so-called GALA method.[19] Briefly, it involves fitting a formula that relates experimental QS to the tilt and azimuthal rotation angles of the peptide, assuming a rigid α-helical conformation. The order of magnitude of the tilts determined using this method is very small, e.g., 5.2° for WALP23 in DMPC and 7.2° for KALP23 in DMPC.[20]

On the other hand, many molecular dynamics (MD) studies have been performed on these model peptides.[21–24] The time scales investigated in these studies varied from 1.5 to 50 ns on either WALP23 or KALP23 peptides. Though the nature or conditions of the simulations were different, all methods predicted tilt angles significantly larger than those determined experimentally by ^{2}H NMR.[20] For example, simulations in an implicit membrane predict a tilt angle of 32.7° for WALP23[22] in a system that has a hydrophobic thickness corresponding to a DMPC bilayer.[25] The first obvious explanation for this discrepancy may be the time scale explored in both computational and experimental works. For a given observable like the tilt angle, which is assumed to be at equilibrium experimentally, the ergodic hypothesis does not hold for short simulations of a few nanoseconds. In addition, if we consider the experimental ^{2}H NMR time scale, which typically is of a few tens of microseconds,[21] there is clearly a limitation from the lack of sampling in such short simulations. The replica exchange technique allowed Im and Brooks to circumvent this problem and even to model the folding and insertion of the peptide;[22] however, the implicit nature of the environment in their study did not allow them to get atomic insights into microscopic lipid/peptide interactions nor precise kinetic details.

The discrepancy between computational and ^{2}H NMR techniques for the tilt angle determination encouraged us to run very long MD trajectories in an explicit environment. Accordingly, we found it interesting to investigate a WALP23 within

an explicit DMPC system that has been very well characterized experimentally[15,26] and that represents a situation of positive though small hydrophobic mismatch. We have chosen to study this system at a peptide-to-lipid (P/L) molar ratio of 1/100, at which no spontaneous peptide aggregation occurs.[27] We analyzed the orientation of the peptide during the trajectories and back-calculated as many parameters as possible to compare MD results with experimental ^{2}H NMR data. Though the lipid parameters and the conformation of the peptide are very well reproduced within the individual trajectories, we find larger tilt angles than in the NMR experiments. However, by applying the GALA method on the quadrupolar splittings back-calculated from several combined trajectories, we retrieve a small averaged tilt angle. On the basis of these results, we propose to interpret the experimental data in a new way and suggest some new experiments to validate our hypothesis.

Methods

Molecular Dynamics of Pure Lipid Systems. MD simulations were performed with GROMACS 3.2.1.[28–30] First simulations were run with pure bilayers using the parameters of Berger,[31] surrounded by single point charge (SPC) water molecules.[32] The starting structure and the parameters were taken from the Web site of Peter Tieleman's group (http://moose.bio.ucalgary.ca/index.php?page=Downloads). The simulation box originally consisting of 128 di-C14:0-PC lipid molecules (64 in each leaflet) and 3655 water molecules was cut at each edge in order to have 118 lipids (59 in each leaflet), leaving 3274 water molecules over (or 27–28 water molecules per lipid). The system was then energy-minimized, and a production run was done for 10–50 ns.

Molecular Dynamics of WALP23/Lipids Systems. For the simulations of the peptide/lipids/water systems, we used the so-called "ffgmx" force field, derived from GROMOS87,[33] that is generally used for peptides/proteins in conjunction with the Berger lipids.[31] First, the peptide was constructed in an ideal α-helix of sequence acetyl-$GW_2(LA)_8LW_2A$-NH_2 ($\phi = -57°$; $\psi = -47°$) and minimized with a few steps of steepest descent. A structure from an equilibrated bilayer of DMPC (after 10–50 ns) was taken in which a hole was created by removing 18 lipids in the center (9 from each leaflet), resulting in a system of 100 lipids. The peptide was then inserted vertically within the bilayer (i.e., along the z-axis, which almost perfectly coincides with the bilayer normal) by adjusting the center of mass of the peptide with that of the bilayer. We thus obtained a system consisting of one WALP peptide, 100 lipids, and 3274 water molecules (32–33 water molecules per lipid), for a total of 14 652 atoms. After a few steps of steepest descent, a 10 ns equilibration was performed by holding the peptide fixed with position restraints (PR) of 1000 kJ·mol^{-1}·nm^{-2} on each heavy atom, while lipids and water were allowed to move normally. For the production runs, the PR were then removed, and simulations of 70–500 ns were performed. One of the runs was started without PR in order to check their influence on the system (see Table 1).

In all simulations, periodic boundary conditions were applied. A 2 fs time step was used for the leapfrog algorithm. All bonds were

(18) de Planque, M. R.; Greathouse, D. V.; Koeppe, R. E., II; Schafer, H.; Marsh, D.; Killian, J. A. *Biochemistry* **1998**, *37*, 9333–9345.
(19) Strandberg, E.; Özdirekcan, S.; Rijkers, D. T.; van der Wel, P. C.; Koeppe, R. E., II; Liskamp, R. M.; Killian, J. A. *Biophys. J.* **2004**, *86*, 3709–3721.
(20) Özdirekcan, S.; Rijkers, D. T.; Liskamp, R. M.; Killian, J. A. *Biochemistry* **2005**, *44*, 1004–1012.
(21) Goodyear, D. J.; Sharpe, S.; Grant, C. W.; Morrow, M. R. *Biophys. J.* **2005**, *88*, 105–117.
(22) Im, W.; Brooks, C. L., III. *Proc. Natl. Acad. Sci. U.S.A.* **2005**, *102*, 6771–6776.
(23) Kandasamy, S. K.; Larson, R. G. *Biophys. J.* **2006**, *90*, 2326–2343.
(24) Petrache, H. I.; Zuckerman, D. M.; Sachs, J. N.; Killian, J. A.; Koeppe, R. E.; Woolf, T. B. *Langmuir* **2002**, *18*, 1340–1351.
(25) de Planque, M. R.; Goormaghtigh, E.; Greathouse, D. V.; Koeppe, R. E., II; Kruijtzer, J. A.; Liskamp, R. M.; de Kruijff, B.; Killian, J. A. *Biochemistry* **2001**, *40*, 5000–5010.

(26) Nyholm, T. K.; Ozdirekcan, S.; Killian, J. A. *Biochemistry* **2007**, *46*, 1457–1465.
(27) Sparr, E.; Ash, W. L.; Nazarov, P. V.; Rijkers, D. T.; Hemminga, M. A.; Tieleman, D. P.; Killian, J. A. *J. Biol. Chem.* **2005**, *280*, 39324–39331.
(28) Berendsen, H. J. C.; van der Spoel, D.; van Drunen, R. *Comput. Phys. Commun.* **1995**, *91*, 43–56.
(29) Lindahl, E.; Hess, B.; van der Spoel, D. *J. Mol. Model.* **2001**, *7*, 306–317.
(30) van der Spoel, D.; Lindahl, E.; Hess, B.; Groenhof, G.; Mark, A. E.; Berendsen, H. J. *J. Comput. Chem.* **2005**, *26*, 1701–1718.
(31) Berger, O.; Edholm, O.; Jahnig, F. *Biophys. J.* **1997**, *72*, 2002–2013.
(32) Berendsen, H. J. C.; Postma, J. P. M.; van Gunsteren, W. F.; Hermans, J. Interaction models for water in relation to protein hydration. In *Intermolecular Forces*; Pullman, B., Ed.; Reidel: Dordrecht, 1981; pp 331–342.
(33) van Gunsteren, W. F.; Berendsen, H. J. C. *Groningen Molecular Simulation (GROMOS) Library Manual*; Biomos: Groningen, 1987.

Table 1. Summary of the Different MD Simulations of the WALP/DMPC/Water System[a]

MD ID	electrostatics treatment	pressure coupling	length (ns)
semiRF	reaction field	semi-isotropic	500 (50)
semiRF2[b]	reaction field	semi-isotropic	150 (50)
semiPME	particle mesh Ewald	semi-isotropic	250 (10)
aniRF	reaction field	anisotropic	150 (10)
aniRF2	reaction field	anisotropic	100 (10)
aniPME	particle mesh Ewald	anisotropic	70 (10)
concatenated trajectory			1100

[a] All trajectories were preceded by simulations of pure DMPC in water in identical conditions. Their length is shown in parentheses in the last column. [b] This simulation was run without any constraint at the start.

constrained by using the LINCS algorithm,[34] and the water molecules were kept rigid using the SETTLE algorithm.[35] The initial velocities were generated at the desired temperature following a Maxwellian distribution. The simulations were done under the NPT ensemble using the weak coupling method of Berendsen for both temperature and pressure.[36] For the pressure, anisotropic or semi-isotropic coupling was used. The peptide, lipids, and solvent molecules were coupled separately to a temperature bath with a time constant of 0.1 ps. The pressure was coupled to an external bath at 1 bar with a time constant of 1.0 ps and a compressibility of 4.5×10^{-5} bar^{-1}. For the electrostatics, we used two techniques to take into account the long-range interactions beyond the cutoff. First, we used a generalized reaction field (RF)[37] with a 1.0 nm cutoff for the van der Waals interactions, and the nonbonded list was updated every 10 steps. For electrostatics, a cutoff of 1.8 nm and a dielectric constant of 54 were utilized.[38,39] Other simulations using the particle mesh Ewald (PME)[40,41] technique were also done with a cutoff for electrostatics of 1.0 nm, a Fourier spacing of 0.12 nm, and an interpolation order of 4; for these simulations, the van der Waals interactions and the nonbonded list were treated similarly to the RF simulations. Anézo et al. showed that the RF may be used for calculating electrostatics of lipid simulations and that it was possible to reproduce results obtained with the classical PME.[42] Our simulations were performed in both RF and PME conditions in order to provide these simulations with a mutual control experiment and because a PME treatment of electrostatics requires more computational time due to scaling problems with the 3.2.1 version of GROMACS. All simulations are presented in Table 1.

The simulations were performed in parallel on a LINUX cluster (Intel Xeon 2.4 GHz processors) or on Power4 P690 CPUs (1.3 GHz) at the French national supercomputer center, IDRIS (Orsay, France). As a CPU cost indication, 1 ns took about 6 h for the simulations using RF on our LINUX cluster on 4 CPUs, and ∼8 h for the PME simulations on 16 CPUs at IDRIS, for a total time of approximately 225 CPU days.

In this paper, we refer to the MD ID as mentioned in Table 1. The concatenated trajectory, as indicated in the last line of Table 1, was obtained by concatenating each simulation without their first 20 ns, in order to have the system relaxed from the initial conditions, especially the release of the PR. This global trajectory allowed us to get more sampling for calculating various averages.

(34) Hess, B.; Bekker, H.; Berendsen, H. J. C.; Fraaije, J. G. E. M. *J. Comput. Chem.* **1997**, *18*, 1463−1472.
(35) Miyamoto, S.; Kollman, P. A. *J. Comput. Chem.* **1992**, *13*, 952−962.
(36) Berendsen, H. J. C.; Postma, J. P. M.; DiNola, A.; Haak, J. R. *J. Chem. Phys.* **1984**, *81*, 3684−3690.
(37) Tironi, I. G.; Sperb, R.; Smith, P. E.; van Gunsteren, W. F. *J. Chem. Phys.* **1995**, *102*, 5451−5459.
(38) Hunenberger, P. H.; van Gunsteren, W. F. *J. Chem. Phys.* **1998**, *108*, 6117−6134.
(39) Smith, P. E.; van Gunsteren, W. F. *J. Chem. Phys.* **1994**, *100*, 3169−3174.
(40) Darden, T.; York, D.; Pedersen, L. *J. Chem. Phys.* **1993**, *98*, 10089−10092.
(41) Essmann, U.; Perera, L.; Berkowitz, M. L.; Darden, T.; Lee, H.; Pedersen, L. G. *J. Chem. Phys.* **1995**, *103*, 8577−8593.
(42) Anézo, C.; de Vries, A. H.; Höltje, H.-D.; Tieleman, D. P.; Marrink, S. J. *J. Phys. Chem. B* **2003**, *107*, 9424−9433.

Trajectory Analysis. Almost all analyses were done using the programs within the GROMACS package, except for a few parameters described herein. The tilt angle is defined as the angle between the helix axis and the normal to the membrane. We calculate the helix axis by taking the first eigenvector of the inertia matrix (defined by all heavy atoms of the backbone). Alternatively, it is possible to choose different parts of the sequence to calculate the axis; unless stated otherwise, we used the sequence defined from Trp3 to Trp21. The normal to the membrane was taken as the z-axis. For the azimuthal rotation (the rotation of the peptide around its main axis), we define it as in ref 20: it corresponds to the angle given by the direction of the tilt with respect to a vector orthogonal to the helix axis that passes through the Cα of Gly1. The anticlockwise direction is taken as positive. Because tilt and rotation calculated in this way are the true angles directly observed from the coordinates, we refer to "real" (or "sim") tilt and azimuthal rotation throughout the paper. For both angles, we developed in-house programs in C within the GROMACS package (namely g_tilt and g_rotation); they are available upon request from the authors or at the URL http://condor.ebgm.jussieu.fr/∼fuchs/download/.

GALA Method Applied to MD Data. The so-called GALA method consists basically in fitting experimental (or simulated) alanine-d_3 ^{2}H NMR quadrupolar splittings (QS) to a tilted α-helix. This procedure applied to MD data is explained here.

The simulations of ^{2}H NMR QS ($\Delta\nu_q$, kHz) of the eight alanine positions between the Trp-residues labeled positions were based on the C$_\alpha$−C$_\beta$D$_3$ bond coordinates, which correspond to the ^{2}H NMR signals that would arise from the deuterons of the alanine side-chain methyl group in NMR experiments.[19] The simulated QS $\Delta\nu_q^i$(sim) values were computed using the equation

$$\Delta\nu_q^i(\text{sim}) = \tfrac{3}{4} K\langle 3\cos^2\theta_i - 1\rangle \qquad (1)$$

where θ_i is defined as the angle between a hypothetical magnetic field taken as the Z axis (NMR experiments described in refs 19 and 43 make use of macroscopically oriented samples with their normal oriented parallel to the magnetic field; the normal to the bilayer in our system coincided very well with the z-axis) and the C$_\alpha$−C$_\beta$ bond of the alanine i.[43] The angular brackets $\langle \cdots \rangle$ corresponded to an ensemble average over all the conformations generated in the MD trajectory (as in ref 21). Alternatively, it is possible to calculate a $\Delta\nu_q^i$(sim) on a single conformation of the MD trajectory. The constant K is defined as

$$K = (e^2 qQ/h)S \qquad (2)$$

where $e^2 qQ/h$ is the quadrupolar coupling constant and S is an order parameter that accounts for molecular motion. In this study, a K value of 49 kHz was used, as in the ^{2}H NMR studies.[43]

From the above ^{2}H NMR quadrupolar splittings, it is possible to evaluate the peptide orientation using the GALA method.[19] For this purpose we used the following equations:

$$\Delta\nu_q^i(\text{GALA}) = \tfrac{3}{4} K(3\cos^2\epsilon_{||}^i(\cos\tau - \sin\tau\cos\delta_i\tan\epsilon_{||}^i)^2 - 1) \quad (3)$$

where τ is the tilt angle, defined as the angle between the peptide helical axis and the bilayer normal, and $\epsilon_{||}^i$ is the angle between the peptide helix axis and the C$_\alpha$−C$_\beta$D$_3$ bond vector of alanine i. δ_i has three components:

$$\delta_i = \rho + \epsilon_{\perp}^i + \varphi_i \qquad (4)$$

where ρ is the (azimuthal) rotation around the helical axis of the C$_\alpha$ of Gly1 with respect to the direction of the tilt (as calculated in the previous section), $\epsilon_{\perp}^i$ is the angle of a vector from the peptide axis to the C$_\alpha$ of

(43) van der Wel, P. C.; Strandberg, E.; Killian, J. A.; Koeppe, R. E., II. *Biophys. J.* **2002**, *83*, 1479−1488.
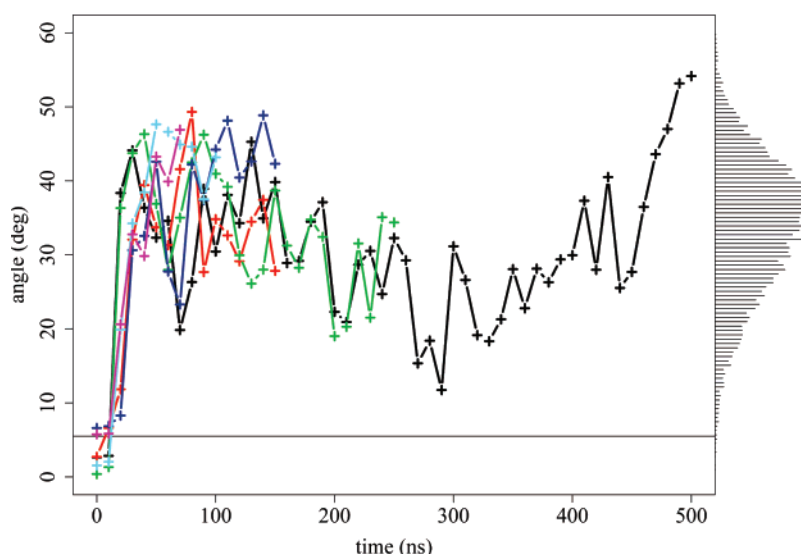
Figure 1. Tilt angle vs time for each simulation (black, semiRF; red, semiRF2; green, semiPME; blue, aniRF; cyan, aniRF2; magenta, aniPME). For clarity, only one point every 10 ns is shown. The solid horizontal line corresponds to the experimental value as determined by ^{2}H solid-state NMR. The bars on the right show the distribution of the tilt for the concatenated trajectory.

alanine i to its bond vector C_α–$C_\beta D_3$ (assumed at $-43.3°$ [19,20]), and φ_i is the twist angle between C_α of the reference Gly1 and C_α of the labeled alanine i. For a regular helix,

$$\varphi_i = -(i-1)\gamma \qquad (5)$$

where i is the residue number and γ is the twist angle between two neighboring residues. In an ideal α-helix, $\gamma = 100°$.

All these angles are described in a scheme in the Supporting Information (see Figure S1) as well as a helical wheel showing the position of the labeled alanines (see Figure S1′).

The principle of the fitting procedure is to make τ, ρ, and $\epsilon_\parallel^i$ vary in order to minimize the root-mean-square deviation (rmsd, kHz) between MD-simulated $\Delta\nu_q^i(\text{sim})$ values (using eq 1) and calculated $\Delta\nu_q^i(\text{GALA})$ (using eq 3):

$$\text{rmsd} = \sqrt{\frac{1}{N_{\text{ALA}}}\sum_{i=1}^{N_{\text{ALA}}}[\Delta\nu_q^i(\text{sim}) - \Delta\nu_q^i(\text{GALA})]^2} \qquad (6)$$

where N_{ALA} is the number of alanines considered in the calculation. Unless otherwise stated, we used the eight alanines of the central leucine–alanine stretch, which gives a regular labeling all around the helical wheel (see Figure S1′). τ, ρ, and $\epsilon_\parallel^i$ were varied for discrete values within the ranges $0–60°$, $0–360°$, and $51–64°$, respectively, using an in-house computer program written in C. This procedure, known as the GALA method, and the way it was derived are described in detail elsewhere.[19,43]

In this paper, we refer to "interpreted" or "GALA_md" tilt/rotation when these angles are deduced from the simulations using the GALA procedure described above, and "real" or "real_md" tilt/rotation when they are evaluated directly from the coordinates of the peptide during the simulation (see previous section). Last, we use "experimental" or "GALA_exp" to refer to the experimental tilt/rotation deduced from the experimental data using GALA.[19,20]

Results

Mutual Effect of WALP23 and Lipids on Each Other. Globally in our simulations, the mutual effect of WALP23 and lipids on each other is in good agreement with experi-

ments.[19,20,25,44] We observe an increase of order when WALP23 is incorporated into the bilayer (see Figure S2), as well as a local increase of the bilayer thickness around the peptide (the two first layers of lipids, see Table S1). In general, the peptide is highly α-helical on the central stretch, with some fluctuations in the extremities. Once, on the semiRF simulation, we observe a major distortion of the helix with the formation of a kink on the N-terminal part, but it is, however, reversible (see Figures S3 and S4). We also find that the peptide is more inserted into the bilayer on the C-terminal side (see Figure S5), which is consistent with some fluorescence spectroscopy and ESR experiments.[27,45,46] The mismatch is globally well alleviated since the difference between the projection of the distance of the hydrophobic stretch (Leu4–Leu20) on the z-axis and the hydrophobic thickness is close to 0 (i.e., -0.4 ± 0.7 Å, see Figure S6).

Apart from these effects, the most dramatic change due to the mismatch is an important reorientation of the peptide within the membrane, which gives rise to a specific behavior of the tilt and azimuthal rotation angles. A detailed analysis of these two angles is presented in the following paragraphs.

Tilt and Azimuthal Rotation Angles. We now look in detail at the precise orientation of the peptide in terms of tilt and azimuthal rotation angles. In Figure 1 is presented the evolution of the tilt angle (real_md) for each simulation. In each trajectory, we observe a fast increase when the peptide is released from the initial positional restraints (PR) at 10 ns, to values around 30° and 40°. The tilt distribution is fairly broad, indicating rather large fluctuations; moreover, the tilt can return to smaller values on a time scale on the order of hundreds of nanoseconds. If we take the longest simulation (black curve), this is the case before 300 ns, after which it goes back to very large values until 500 ns. Interestingly, the tilt appears not to depend on the conditions,

(44) de Planque, M. R.; Kruijtzer, J. A.; Liskamp, R. M.; Marsh, D.; Greathouse, D. V.; Koeppe, R. E., II; de Kruijff, B.; Killian, J. A. *J. Biol. Chem.* **1999**, *274*, 20839–20846.
(45) Naarmann, N.; Bilgicer, B.; Kumar, K.; Steinem, C. *Biochemistry* **2005**, *44*, 5188–5195.
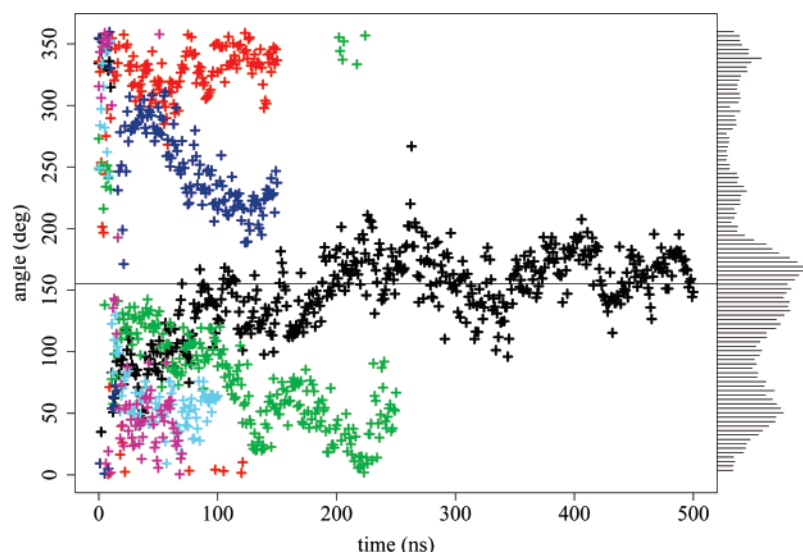(46) Nielsen, R. D.; Che, K.; Gelb, M. H.; Robinson, B. H. *J. Am. Chem. Soc.* **2005**, *127*, 6430–6442.

Figure 2. Azimuthal rotation angle vs time for each simulation (black, semiRF; red, semiRF2; green, semiPME; blue, aniRF; cyan, aniRF2; magenta, aniPME). For clarity, only one point per nanosecond is shown. The solid horizontal line corresponds to the experimental value as determined by ^{2}H solid-state NMR. The bars on the right show the distribution of the rotation for the concatenated trajectory. Note that the very large fluctuations during the first 10 ns are due to the fact the peptide is held vertically; hence, the azimuthal rotation definition is ambiguous.

as the behavior is fairly similar between the different simulations. In any case, we see that, most of the time, the values during our trajectories are by far larger than the experimental (GALA_exp) value of 5.2°.[20]

Figure 2 presents the azimuthal rotation angle (real_md) of each simulation. For each trajectory, the rotation reaches a different value. It converges very slowly, and more than 200 ns is required to reach a stable value; the time scale of equilibration for this parameter is considerably longer than that of the tilt angle. Since we tested two times the reaction field approach for both of our simulations using a semi-isotropic or anisotropic pressure coupling, and each time with different initial velocities, we can conclude that the reached value does not depend on the way we calculate electrostatics nor the way we couple the system to the pressure bath, but rather that it is determined by the initial conditions. The distribution of the rotation angle seems to reveal that there may be some preferred calibrated values; e.g., there are two maxima in the distribution around 50° and 150° and, to a lesser extent, around 250° and 350°. Nevertheless, no preference can be inferred from our simulations since their length is different and their number is not large enough to get good statistics. Interestingly, the longest simulation of 500 ns converges pretty well to the experimental value (i.e., 155°). However, we saw in the preceding section that the tilt angle (real_md) observed in our MD was by far larger than that determined experimentally (GALA_exp). To solve this discrepancy, we further analyze the ^{2}H NMR quadrupolar splittings in the next section.

^{2}H NMR Quadrupolar Splittings. In order to optimally compare our simulations to ^{2}H NMR data,[19,20] we back-calculated the QS (using eq 1 on the concatenated trajectory), $\Delta\nu_q^j$(sim), that would arise if the side chain of alanines were labeled with [2]H. The distributions of QS for each alanine during the concatenated trajectory are plotted in Figure 3 as histograms. The first striking observation is that these distributions are very broad; each alanine covers all the values of QS that are possible (~ -36.7 to 73.5 kHz). This indicates that the angle θ_i of the $C_\alpha - C_\beta$ bond compared to the normal can take several different
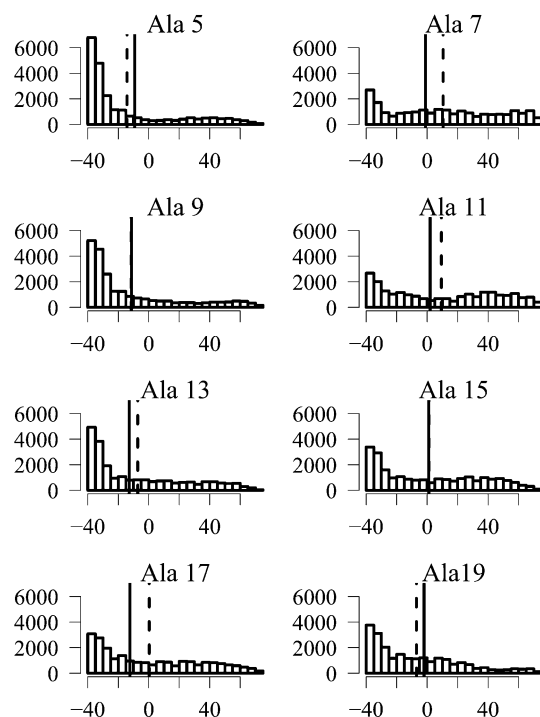

Figure 3. Distribution of simulated ^{2}H NMR quadrupolar splittings for each alanine in the concatenated trajectory. The QS on the x-axis are in kilohertz, whereas the y-axis represents the number of counts in each bin. The vertical solid line represents the experimental value, while the dashed line represents the average over the concatenated trajectory (calculated using eq 1). Note that ^{2}H NMR values can also be negative.

values, e.g., at least from 0 to $\sim 120°$ for each Ala, and even from 0 to almost 180° for Ala15 (data not shown). This broad range of values is explained by the fact that the peptide visits several orientations with different azimuthal rotations among the different trajectories (see the rotation distribution in Figure 2). If only one trajectory is considered, the distribution is much tighter (see Figures S7 and S8 for the distributions of QS on the semiRF and semiPME trajectories, respectively).

The difference between experimental and calculated QS considered in an oriented sample is shown in Table 2 (to get

Table 2. Absolute Deviation $\delta\Delta\nu_q$, in kHz, from Experimental Quadrupolar Splittings for Each Trajectory[a]

	semiRF	semiRF2	semiPME	aniRF	aniRF2	aniPME	concatenated
Ala5	21.7	36.3	17.7	53.4	23.8	17.2	5.0
Ala7	28.5	31.2	25.4	32.1	20.4	2.9	11.5
Ala9	20.2	61.9	6.6	25.8	12.2	2.5	0.3
Ala11	40.9	35.9	3.6	19.9	19.7	25.9	7.3
Ala13	18.1	58.9	14.8	1.2	23.7	38.5	5.6
Ala15	26.9	33.4	23.0	13.3	33.6	33.6	0.2
Ala17	9.8	30.9	37.6	16.0	59.8	63.3	12.7
Ala19	3.9	18.3	28.2	44.2	32.2	31.4	5.0
average	21.3	38.4	19.6	25.7	28.2	26.9	6.0

[a] To evaluate the sign of experimental quadrupolar splittings, eq 3 is used with the tilt and rotation from refs 19 and 20. The deviation is then calculated using $\delta\Delta\nu_q = |\Delta\nu_q(\text{exp}) - \Delta\nu_q(\text{sim})|$ (thus taking the QS sign into account; the experimental (absolute) value itself is taken from ref 19). QS have been considered as in an oriented sample.

the values in an unoriented sample, one has just to divide them by 2). The discrepancy is spectacularly larger if the mean is calculated on a single simulation (from 20 to almost 40 kHz) than on the concatenated trajectory ($\sim$6 kHz). In the case of the concatenated trajectory, there is a clear effect of averaging because the distribution is very broad (see Figure 3). For each QS, it leads to a mean whose absolute value is lower compared to any single simulation. This indicates that it may be worth taking different trajectories to compare our simulation results with the NMR data.

Comparison of the Real and Interpreted Tilt/Rotation. One other way of comparing our simulations to the ^{2}H NMR experiment was to use the same method to derive the peptide orientation—thus the GALA procedure (eq 3)—but with the QS back-calculated from the trajectories (eq 1). In each case, the rmsd was rather low (<3 kHz, see Table S2), which shows that the fit was good. It means that the set of QS back-calculated from the trajectories fits well the orientation found by the GALA procedure. Moreover, this set of rmsd is fairly close to the value 0.9 kHz in the experimental work[19] based on the same number of alanines (eight) (the rmsd of 0.3 kHz in ref 20 was based on only four alanines). One important remark is that the longer the trajectory, the lower the rmsd, and the better the fit. This again shows that it may be worth considering the concatenated trajectory rather than any single one to derive the peptide orientation.

A comparison of the interpreted (GALA_md), experimental (GALA_exp),[20] and real (real_md) tilt and rotation angles is presented in Table 3 (see Methods for a precise definition of these angles). Let us focus first on the tilt. As can be seen in Table 3 and Figure 1, the tilt is always a lot larger when evaluated from individual simulations by either method (real_md or GALA_md) compared to the experimental one (GALA_exp). Of particular importance is the fact that the interpreted tilt (GALA_md) is systematically smaller than when measured from the coordinates of the peptide (real_md). This comes from the fact that the interpreted tilt (GALA_md) is calculated from the QS averaged over the whole length (except the first 20 ns) of each simulation (using eq 1). Therefore, if the rotation undergoes some important variations and/or fluctuations, the QS will populate a broader distribution within their possible range ($\sim$ -36.7 to 73.5 kHz) and tend to get averaged toward small values, which are compatible with small tilts. Thus, the absolute value of QS decreases, leading somehow to a smaller interpreted tilt (GALA_md) (because small tilts correspond to small QS in eq 3, whatever the rotation). When we calculate the tilt by the GALA procedure on windows of 10 ns, the value is closer to

Table 3. Comparison of Experimental, Interpreted, and Real Tilt and Azimuthal Rotation Angles[a]

simulation	interpreted (GALA_md)	real (real_md)	experiment (GALA_exp)
Tilt			
semiRF	22.3[b]	31.2 ± 9.6	
semiPME	19.7	32.8 ± 7.0	
semiRF2	29.4	33.9 ± 7.5	
aniRF	26.1	37.1 ± 9.6	5.2
aniPME	27.4	37.7 ± 7.2	
aniRF2	31.1	40.6 ± 6.2	
concatenated	6.5[b]	33.5 ± 9.0	
Rotation			
semiRF	145[b]	139 ± 28	
semiPME	60	70 ± 38	
semiRF2	321	331 ± 19	
aniRF	245	248 ± 31	155
aniPME	30	45 ± 27	
aniRF2	47	55 ± 16	
concatenated	106[b]	153[c] ± 91	

[a] All angles are expressed in degrees; for each single trajectory, angles or QS were averaged from 20 ns to the end of the simulation. [b] Calculated on all alanines except Ala5 because of the kink occurrence. [c] This mean has been obtained considering the rotation range between 0° and 360°.

the real one (see Figure S9), because it does not have time to be significantly averaged. The most spectacular result of this averaging effect is the case of the concatenated trajectory. We find a value for the interpreted tilt (GALA_md) of 6.5°, which is very close to the experimental interpreted one (GALA_exp) (5.2°).[20] However, this is significantly smaller than the 33.5° found for the real tilt (real_md). Bearing in mind that the length of the concatenated trajectory is 1.1 μs, thus about 1 order of magnitude below the NMR time scale, and that we used different initial conditions as may be the case if several peptides are present, like in a macroscopic experiment, we can propose that this trajectory is close to what may happen in the NMR experiment. Therefore, we propose that the 5.2° interpreted from NMR data (GALA_exp) may be the result of a rude averaging (over the time scale and over all the labeled molecules of the macroscopic sample), and thus higher tilt angles are likely to occur.

If we now focus on the rotation, we see that the interpreted (GALA_md) and real (real_md) values are very close (up to 10°) if one single simulation is considered. The standard deviation around 30° comes from the time rotation takes to converge. However, we see that the agreement for the concatenated trajectory is not as good as for a single trajectory. For the real rotation (real_md), the mean value depends on whether we consider the range 0/360 or $-180/180$; using this former range as in ref 20, we retrieve a value very close to the

experimental interpreted one (GALA_exp). However, the large standard deviation of 91° reflects well the fact that rotation visits several different values (see also the distribution in Figure 2). In fact, these large fluctuations are responsible for the averaging of QS and thus for the small tilt angle when it is calculated by the GALA method. This shows that the results of this procedure can lead to values of tilt and rotation that are the results of averaging effects. The results of our simulations suggest that some other substates may exist that give rise to the overall tilt and rotation obtained by the GALA method from experimental data. MD appears, therefore, as a good tool to probe those substates.

Discussion

In this work, we have used MD simulations to investigate how the WALP23 peptide orients itself under a small hydrophobic mismatch within DMPC lipids. So far, to our knowledge, this is the longest set of simulations ever done on a single transmembrane peptide in one given explicit lipid/water environment. The starting configuration of our simulations was such that the peptide hydrophobic stretch was longer than the hydrophobic bilayer thickness. Globally, the response to this hydrophobic mismatch in our simulations comes from two main mechanisms. First, we observed a local increase of the hydrophobic thickness of the phospholipid bilayer around the peptide, especially the two first layers of lipids. Second, the peptide undergoes important reorientations once put within the bilayer: first it presents a large tilt angle, and thereafter, it seems to take some specific azimuthal rotations. Interestingly, we could observe that the (real) tilt angle was slightly correlated to the bilayer thickness of the lipids around the peptide (see close lipids in Table S1 and Figure S10). This suggests that the tilt angle decreases simultaneously with increasing bilayer thickness. Of course, this adaptation is only a trend, as there are enormous fluctuations; nevertheless, it is reproducible, as we observed it in all simulations. All these results are in good agreement with solid-state NMR experiments.[47]

One important aspect of our study reveals insights into the dynamic behavior of the azimuthal rotation angle. To our knowledge, the only MD study that analyzed the azimuthal angle of model transmembrane peptides so far was performed on a Lys-flanked KALP-like peptide.[21] The comparison with experimental QS was pretty good, probably due to a good match between the QS of the starting conformation and the experimental ones. However, the azimuthal rotation did not show a clear convergence due to the short simulation time (10 ns). Moreover, it is hardly comparable to our work, since the flanking residues, which have been shown to influence the azimuthal rotation,[20] are different. In our simulations, we observed that the rotation angle (real_md) takes a long time to reach a stable value, and only the very long simulation (semiRF) showed a relative convergence. This means that adopting the final rotation angle has a relaxation time on the time scale of hundreds of nanoseconds. Interestingly, the longest simulation of 500 ns converged pretty well to the experimental interpreted value (GALA_exp). One other important aspect is that the obtained rotation angle on a given simulation depends on the initial conditions. This is probably due to the fact there is a significant

free energy barrier to rotation once the peptide is significantly tilted. Thus, for a given set of initial velocities, the peptide is trapped at a specific rotation. This shows that the sampling is definitely not sufficient to reach any equilibrium if we consider a single simulation, especially if it is only a few nanoseconds long. This implies that it is mandatory to run several different long simulations to tackle this problem. We see that even though the present work is the largest sampling ever simulated on a transmembrane peptide under a given set of conditions (1.1 μs), it seems not enough to unambiguously answer the question, "What is the average rotation?" It would be interesting to prolong all simulations to 500 ns (or even more) to assess this question of convergence. Another way to get clues on this point would be to compute a 2D potential of mean force vs tilt and rotation. However, this would require a huge amount of computation resources if atomistic simulations were to be used. Coarse-grained approaches would probably be better suited to reach such time scales and to circumvent sampling issues.

In this work, we find pretty high real tilt angles (real_md) compared to the NMR experiments (GALA_exp).[19,20] In literature, almost all MD dealing with (W/K)ALP23 peptides in explicit (atomistic or coarse-grained) or implicit solvent revealed higher tilt angles than the 5.2°/7.2° estimated experimentally in similar mismatch conditions.[21−24,48−50] We discuss now possible explanations for the discrepancy between experimental and computational works reporting on the peptide orientation.

We showed that the system was highly dynamical and that care had to be taken to interpret experimental data, especially at the level of the peptide orientation. The best way for this purpose was to back-calculate the QS from our simulations (using eq 1) and compare them directly to the experimental values. We saw that the agreement was definitely better if the averaging was done on the concatenated trajectory instead of a single one. Since the range of values of QS (in an oriented sample) is from $\sim$ −36.7 to 73.5 kHz, and many different orientations are visited among the different trajectories, these latter values tend to be averaged toward small (absolute) values. It follows that the tilt angle found using the GALA procedure (eqs 3 and 4) will tend to small values (6.5°), as small tilt angles give rise to small QS in eq 3. This means that the ensemble represented by our concatenated trajectory fits pretty well the experimental data, though the observed (real_md) tilt calculated from the peptide coordinates is rather high (33.5°) compared to the experimental one (GALA_exp) (i.e., 5.2°[20]). We thus propose that experimental QS could represent an average of many different orientations, including tilt angles higher than 5.2°, and important fluctuations in the azimuthal rotation angles. This means that the interpreted tilt angle in the experiments (GALA_exp) is probably underestimated compared to the real situation. Nevertheless, an experimental validation is needed to confirm this hypothesis. We briefly review, in the following, experimental techniques dealing with the determination of the extent of tilt.

In the literature, some other experimental works give tilt angles higher than 5.2° on mismatch situations similar to the

(47) Özdirekcan, S.; Nyholm, T.; Raja, M.; Rijkers, D.; Liskamp, R.; Killian, J. A. *Biophys. J.* **2007**, in press.

(48) Bond, P. J.; Holyoake, J.; Ivetac, A.; Khalid, S.; Sansom, M. S. *J. Struct. Biol.* **2007**, *157*, 593−605.
(49) Ramamoorthy, A.; Kandasamy, S. K.; Lee, D. K.; Kidambi, S.; Larson, R. G. *Biochemistry* **2007**, *46*, 965−975.
(50) Sengupta, D.; Meinhold, L.; Langosch, D.; Ullmann, G. M.; Smith, J. C. *Proteins* **2005**, *58*, 913−922.

present one. de Planque et al. found ~10−15° for WALP23 in DMPC using ATR-FTIR.[25] The relationship between the peptide hydrophobic length and the tilt angle in this study was not as clear as with ^{2}H NMR.[20] Opella's group found a tilt of 27° for the transmembrane helix of Vpu in di-14:0-PC lipids, using PISEMA experiments based on ^{15}N solid-state NMR.[51] Using similar experiments in DMPC, Larson's group retrieved tilt angles of 25−30° for some cell signaling peptides, which was also confirmed by MD.[49] On the other hand, most of the studies that used ^{2}H NMR with the GALA technique on transmembrane peptides reported systematically small tilt angles.[19,20,43,52] In view of all these examples, our work suggests that it may be worth doing new experiments using both [2]H (GALA) and ^{15}N (PISEMA) solid-state NMR techniques, but on exactly the same systems under similar conditions (same peptide, phospholipids, concentration, P/L ratio, temperature, extent of hydration, buffer composition, etc.).

Apart from this confirmation by another NMR experiment, it would be interesting to improve the GALA method by taking the rotation fluctuations into account. In its actual version, the GALA procedure is appropriate for the determination of the averaged rotation angle from the experimental QS, which are averages themselves. It seems, however, impossible to determine unambiguously the extent of tilt angle since we can find the same tilt whatever the fluctuations of QS are, as long as their mean is the same. But the ^{2}H NMR experiment gives access only to the average QS, not to the instantaneous fluctuations. It is thus impossible to determine the fluctuations of rotation experimentally on the NMR time scale. Such fluctuations might be determined from multiple MD simulations, but as discussed above, some complementary works are still needed to get a reliable average. Furthermore, it would probably be important to test the effect of the force field choice on these fluctuations. At present, MD seems well suited to complement ^{2}H NMR experiments in the determination of peptide orientation, since it allows the dynamics to be taken into account, even if some further tests are still necessary.

In conclusion, our work gives useful insights into the interpretation of the peptide orientation from experimental data and gives molecular details of the system. It is a good example of what computational techniques can bring to the experiments. This also demonstrates the need to run rather long simulations or, more generally, to generate enough sampling in order to overlap or go beyond the experimental time scale. We believe that the improvement of new accurate coarse-grained force fields will allow the simulation community to reach time scales that go over the experimental one.

Note Added in Proof. After this article was submitted, a similar MD study on WLP23 and KLP23 was published (Esteban-Martin, S.; Salgado, J. *Biophys. J.* **2007**, in press). Using multiple simulations of 200 ns for each peptide, the authors observed the same phenomenon as we did, that is, averaging effects of the back-calculated quadrupolar splittings lead to small tilt angles when they are evaluated with the GALA method.

Supporting Information Available: Definition of angles used in the GALA method, helical wheel representation of WALP23, experimental and MD back-calculated ^{2}H NMR order parameter profiles, bilayer thickness of pure DMPC or DMPC/WALP23 systems, evolution of WALP23 secondary structure, snapshots of WALP23 in a DMPC bilayer, density profiles of different groups of the DMPC/WALP23 system, distribution of the difference between the hydrophobic thickness and the projection of the length of the peptide's hydrophobic stretch on the *z*-axis, distribution of simulated ^{2}H NMR quadrupolar splittings for each alanine in the semiRF and semiPME trajectories, detailed results of the GALA procedure on each trajectory, comparison of the real_md and GALA_md tilt angles for the semiRF simulation, and tilt angles versus the hydrophobic bilayer thickness. This material is available free of charge via the Internet at http://pubs.acs.org.

JA073784Q

(51) Park, S. H.; Opella, S. J. *J. Mol. Biol.* **2005**, *350*, 310−318.
(52) Gibbons, W. J., Jr.; Karp, E. S.; Cellar, N. A.; Minto, R. E.; Lorigan, G. A. *Biophys. J.* **2006**, *90*, 1249−1259.